

Aging of orientation fluctuations in stripe phases

Christian Riesch, Günter Radons, and Robert Magerle

Institut für Physik, Technische Universität Chemnitz, D-09107 Chemnitz, Germany

(Received 1 July 2014; published 3 November 2014)

Stripe patterns, observed in a large variety of physical systems, often exhibit a slow nonequilibrium dynamics because ordering is impeded by the presence of topological defects. Using computer simulations based on a well-established model for stripe formation, we show that a slow dynamics and aging occur also in stripe patterns free of topological defects. For a wide range of noise strengths, the two-time orientation correlation function follows a scaling form that is typical for systems exhibiting a growing length scale. In our case, the underlying mechanism is the coarsening of orientation fluctuations, ultimately leading to power-law spatial correlations perpendicular to the stripes. Our results show that even for the smallest amount of noise, stripe phases without topological defects do not reach equilibrium. This constitutes an important aspect of the dynamics of modulated phases.

DOI: [10.1103/PhysRevE.90.052101](https://doi.org/10.1103/PhysRevE.90.052101)

PACS number(s): 05.40.-a, 61.20.Lc, 89.75.Kd, 64.75.Gh

I. INTRODUCTION

The formation of spatially extended patterns is a complex and much-studied phenomenon [1]. In particular, stripe patterns are observed in physical systems as diverse as block copolymers [2], thin magnetic films [3], and high- T_c superconductors [4], as well as Rayleigh-Bénard convection [5]. Stripes can be described as a density profile which is periodic in only one spatial dimension. Such systems are known to be strongly influenced by fluctuations, especially in low dimensions [6]. A question which has not been considered before is how stripe patterns approach equilibrium, starting from an ordered state under the influence of noise. The aging effect, where important properties of a system strongly depend on the waiting time, is well known from the study of glassy systems [7], which by definition do not reach thermal equilibrium. Although glasses are ubiquitous in nature, the glass transition and the associated slow dynamics are still not completely understood [8,9]. In trying to model glasses, much effort has been spent investigating systems with self-generated as well as quenched disorder [10,11]. The picture that has emerged is one of a rugged energy landscape in configuration space, where a system evolves between a large number of local minima. Quenched disorder, however, is not a requirement for the observation of a glassy dynamics and aging [12]. For instance, domain growth is one scenario where aging is observed [13,14]. Certain stripe-forming systems do exhibit domain growth, with domains consisting of regions of parallel stripes [15–17]. Some aspects of glassy dynamics have been identified in the process of domain coarsening in one [18] and two spatial dimensions [19]. In the latter work, the pinning of grain boundaries was reported to lock the system in a state lacking long-range order. Using replica calculations, Schmalian and Wolynes have been able to show that a particular model for stripe formation exhibits a glass transition due to the emergence of an exponentially increasing number of metastable states [20]. Their work, as well as a later study specific to block copolymers [21], did not address the dynamics of the system. On the other hand, the slow relaxation after a quench within the ordered

lamellar phase has been investigated using a linear stability analysis [22].

In this work, we use computer simulations based on a well-established model for a stripe-forming system to investigate the slow orientational dynamics of stripes in the ordered state. We will show below that even a small amount of noise gives rise to small-angle orientation fluctuations which exhibit aging, as revealed by investigating the two-time autocorrelation functions. Topological defects and metastable states, which are often associated with slow dynamics, are not responsible for the aging effects we observe. This result has important implications for the interpretation of the thermodynamics of stripe phases. More generally, our results emphasize the importance of small shape fluctuations for the slow dynamics of modulated phases [23].

II. MODEL AND METHODS

As a model system, we study the well-known model B [24] with Coulomb interactions. The dynamic equation is

$$\frac{\partial \psi}{\partial t} = \nabla^2 \frac{\delta \mathcal{F}}{\delta \psi} + \xi, \quad (1)$$

where the scalar field $\psi(\mathbf{r}, t)$ represents, for example, a conserved magnetic quantity or the concentration difference $\psi_A - \psi_B$ between two species A and B . \mathcal{F} is the free-energy term introduced by Ohta and Kawasaki for modeling diblock copolymer melts below the critical temperature [25]:

$$\mathcal{F}[\psi] = \int d^d r \left\{ -\frac{\psi(\mathbf{r}, t)^2}{2} + \frac{\psi(\mathbf{r}, t)^4}{4} + \frac{1}{2} [\nabla \psi(\mathbf{r}, t)]^2 \right\} + \frac{\Gamma}{2} \iint d^d r' \psi(\mathbf{r}', t) G(\mathbf{r}', \mathbf{r}) \psi(\mathbf{r}, t) d^d r, \quad (2)$$

where d is the dimension of the system and $G(\mathbf{r}, \mathbf{r}')$ is defined by $\nabla^2 G(\mathbf{r}, \mathbf{r}') = -\delta(\mathbf{r} - \mathbf{r}')$. The first integral in Eq. (2) is the usual Ginzburg-Landau term, whereas the second integral describes long-range Coulomb interactions. $\xi(\mathbf{r}, t)$ is Gaussian white noise characterized by $\langle \xi(\mathbf{r}, t) \rangle = 0$ and

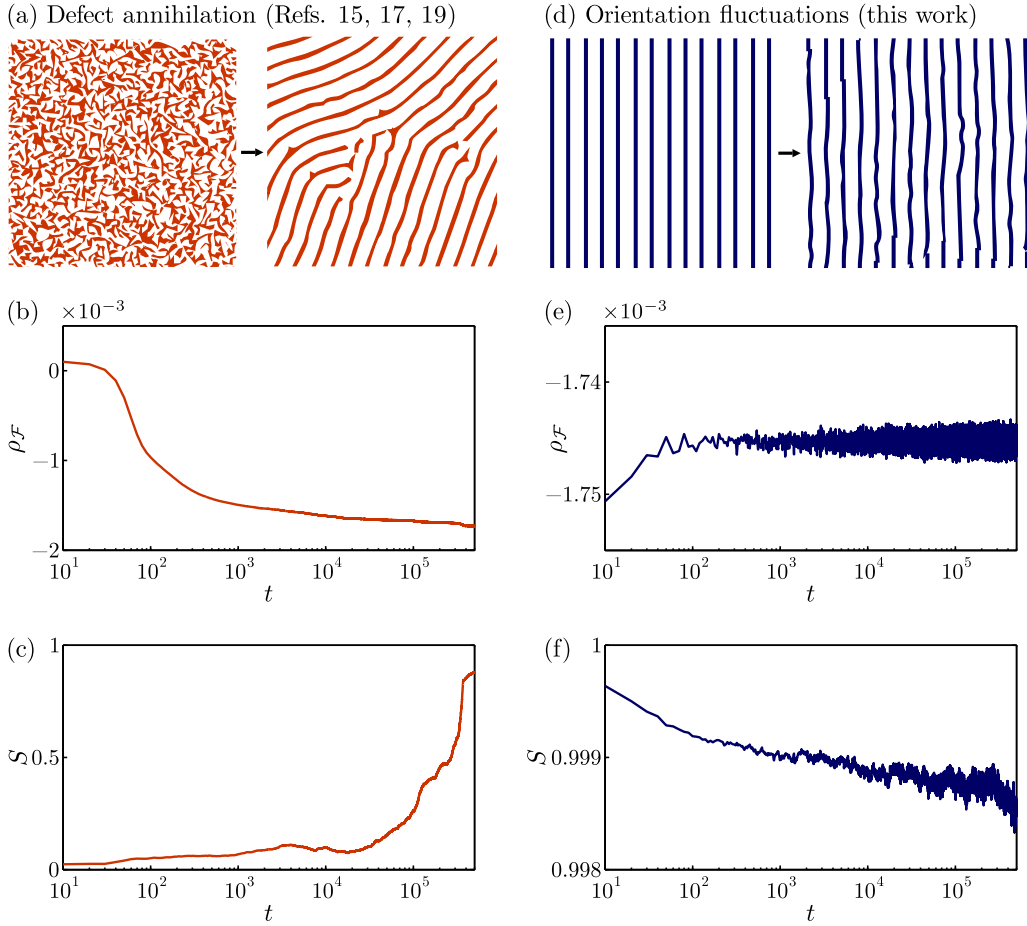


FIG. 1. (Color online) Two types of slow dynamics in stripe patterns starting from different initial conditions. (a)–(c) Homogeneous initial state. (d)–(f) Striped initial state. The noise strength $\eta/\eta_c = \frac{1}{30}$ in both cases. (a) and (d) show binarized snapshots representing the corresponding dynamics of the concentration field $\psi(\mathbf{r}, t)$. The free-energy density $\rho_{\mathcal{F}}(t)$ decays slowly for homogeneous initial conditions (b), whereas it becomes stationary in the ordered system (e). During defect annihilation, the orientational order parameter $S(t)$ remains close to zero for a long time, but approaches unity at later times (c). In contrast, the ordered system exhibits a very slow but ongoing decay of $S(t)$ (f).

$\langle \xi(\mathbf{r}, t) \xi(\mathbf{r}', t') \rangle = -2\eta\delta(t - t')\nabla^2\delta(\mathbf{r} - \mathbf{r}')$, where $\langle \cdot \rangle$ stands for the statistical average and η parameterizes the noise strength. While this model describes a conserved quantity $\psi(\mathbf{r}, t)$ and contains long-range interactions, none of these properties are essential for the dynamics described below, as shown by further results [26] for the conserved and nonconserved Swift-Hohenberg equation [27]. The aforementioned models are all examples for a class of systems first discussed by Brazovskii [28].

The equation obtained by inserting Eq. (2) into Eq. (1) has been widely used in numerical studies of the microphase separation and microdomain ordering in block copolymers [29–33], and continues to be used today [34–37]. The same model also describes reactive binary mixtures [38,39]. Recently, it has been used to study the possible applications of block copolymer thin films as lithographic resists [40–42]. There is also a large body of work concerning Coulomb-frustrated ferromagnets [43–45]. For further applications of this model, see Ref. [46]. For $\Gamma = 0$, the model describes the macrophase separation for a conserved order parameter, namely, spinodal

decomposition [13,47]. The system forms stripes within the range $0 < \Gamma < \frac{1}{4}$ [15]. The influence of additive noise on stripe patterns has been investigated to some extent in previous works [48–51]. For a given value of Γ , a critical noise level η_c exists which marks an order-disorder transition (ODT) [48]. In our case, $\eta_c = 0.020(3)$. The properties of the ODT are not central to this work, as we focus on the behavior in the ordered phase far below the critical noise strength.

We have numerically solved Eqs. (1) and (2) for $d = 2$ on a square lattice of size $L \times L$, with $L = 517$ and a lattice spacing $\Delta x = 1$, using a pseudospectral algorithm with a third-order scheme for the time integration [52] and periodic boundary conditions. We have also checked the validity of our results for larger systems up to $L = 1710$. The initial conditions were parallel stripes given by $\psi(x, y) = A \cos(kx)$. The amplitude A and wave number k were computed using this single-mode approximation by minimizing the free energy, yielding $A = 2\sqrt{(1 - 2\sqrt{\Gamma})/3}$ and $k = \Gamma^{1/4}$ [39]. The time step $\Delta t = 0.1$ and $\Gamma = 0.2$ were kept constant in all simulations. The values for L were chosen to be commensurable with the

stripes' wavelength $\lambda \approx 9.4$, but a small mismatch as well as global rotation of the system have no significant influence on the results presented below. The local stripe orientation $\theta(\mathbf{r}, t)$, commonly used to investigate the physics of stripe patterns [15,16,53], was computed using the gradient-square tensor implemented in reciprocal space [54].

III. RESULTS

A. Types of slow dynamics

The dynamics observed in the stripe-forming system is largely determined by the initial conditions. Usually, a homogeneous state is prepared that represents a high-temperature mixture of the two components. The evolution is then followed after quenching to a region of the phase diagram where the mixed state is unstable [29]. In this work, we focus on the relaxation from a completely ordered state, that is, a pattern of parallel stripes, with a finite noise strength. Some examples of the evolution resulting from the two different initial conditions are shown in Fig. 1. The free-energy density $\rho_{\mathcal{F}} \equiv \mathcal{F}[\psi]/L^2$ quickly decreases for $0 < t \lesssim 500$ in the case of homogeneous initial conditions, which is associated with stripe formation, but the subsequent evolution is slow. At late times, the orientational order parameter $S(t) \equiv |\langle e^{2i\theta(\mathbf{r}, t)} \rangle_{\mathbf{r}}|$ approaches unity, as most defects in the system have been annihilated. In contrast, the free-energy density of an ordered system initially increases slightly for $t \lesssim 100$, as the pattern is perturbed by the noise, and then remains constant. The apparent growth of fluctuations in $\rho_{\mathcal{F}}$ is an effect of displaying the data on a logarithmic time scale. The orientational order parameter $S(t)$ remains close to unity at all times, but does not reach a stationary value. While the slow dynamics caused by domain growth and annihilation of topological defects is well known [15,17,19,55], our results show that there is also a slow relaxation taking place in the ordered stripe pattern. This relaxation entails subtle changes in the stripe pattern. Figure 2 shows snapshots of the concentration field $\psi(\mathbf{r}, t)$ and the corresponding orientation field $\theta(\mathbf{r}, t)$ at a late stage of the evolution. The stripes formed by $\psi(\mathbf{r}, t)$ are visibly distorted by the noise, with neighboring stripes showing similar deviations. This is more fully revealed by the orientation field $\theta(\mathbf{r}, t)$, where elongated domains appear perpendicular to the stripes [56]. Below, we will relate these structures to growing spatial correlations in $\theta(\mathbf{r}, t)$. Note that the orientation field of the block-copolymer stripe pattern measured in Ref. [57] is very similar to the one depicted in Fig. 2(b).

B. Fluctuations of ordered stripes

We will now analyze the fluctuation dynamics of the ordered stripe pattern by computing the two-time correlation functions of the concentration field and the orientation field. The concentration autocorrelation function is defined by $C_{\psi}(t, t_w) \equiv \langle \psi(\mathbf{r}, t) \psi(\mathbf{r}, t_w) \rangle_{\mathbf{r}, \xi}$, where $t_w \leq t$ is the waiting time and $\langle \cdot \rangle_{\mathbf{r}, \xi}$ represents averaging over the spatial locations \mathbf{r} and independent noise realizations ξ , respectively. The spatial average $\langle \psi(\mathbf{r}, t) \rangle_{\mathbf{r}}$ vanishes at all times. The orientation corre-

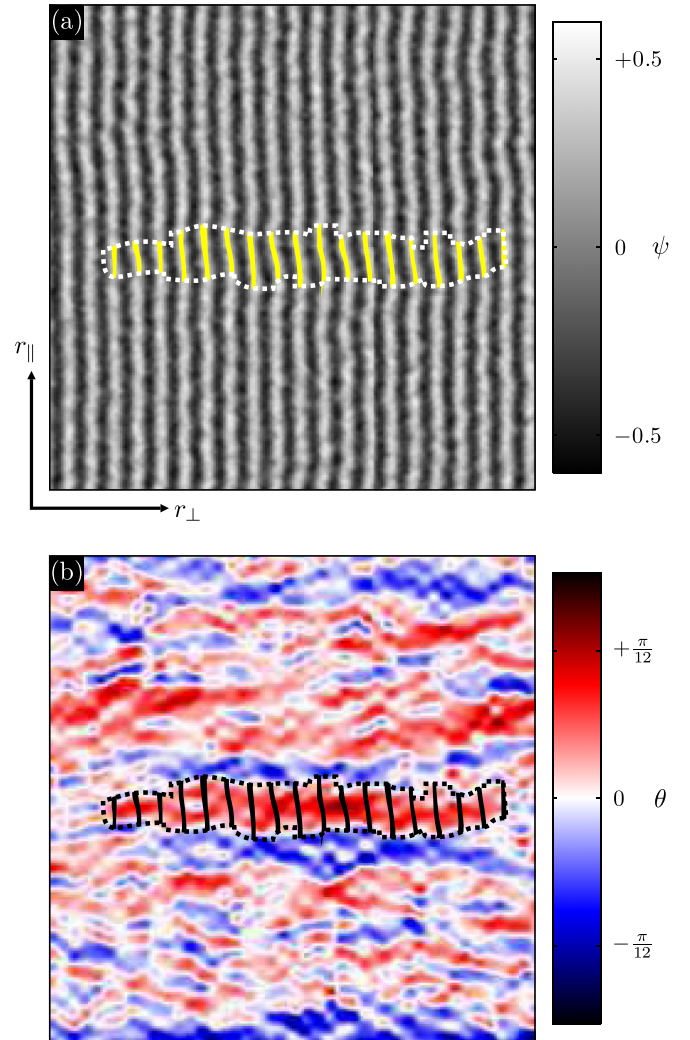


FIG. 2. (Color online) Orientation fluctuations within the ordered stripe pattern at late times. (a) Concentration profile $\psi(\mathbf{r}, t = 5.2 \times 10^5)$ for $\eta/\eta_c = \frac{1}{3}$. (b) The corresponding orientation field $\theta(\mathbf{r}, t = 5.2 \times 10^5)$. The centers of stripes forming an orientational domain extending perpendicularly to the stripes are marked in (a) and (b). The snapshots are sections 200×200 in size of a system with $L = 517$. The further temporal evolutions of these patterns are shown in the videos S1 and S2, respectively (see Supplemental Material [56]).

lation function is given by $C_{\theta}(\mathbf{r}, \mathbf{r}', t, t') \equiv \langle e^{2i[\theta(\mathbf{r}, t) - \theta(\mathbf{r}', t')]} \rangle_{\xi} - \langle e^{2i\theta(\mathbf{r}, t)} \rangle_{\xi} \langle e^{-2i\theta(\mathbf{r}', t')} \rangle_{\xi}$, taking into account the nematic symmetry of the stripe orientation. We will use two derived quantities, the autocorrelation function $C_{\theta}(t, t_w) \equiv \text{Re} \langle C_{\theta}(\mathbf{r}, \mathbf{r}, t, t_w) \rangle_{\mathbf{r}}$ and the spatial correlation function $C_{\theta}(\mathbf{r}, t) \equiv \text{Re} \langle C_{\theta}(\mathbf{r}', \mathbf{r}' + \mathbf{r}, t, t) \rangle_{\mathbf{r}'}$. The data shown here have been averaged over 40 independent simulation runs for $\eta < \eta_c$ and 5 runs for $\eta > \eta_c$.

First we plot the autocorrelation functions as functions of the time difference $t - t_w$ to check for time-translation invariance and thus for stationarity in the dynamics (Fig. 3). The concentration autocorrelation function $C_{\psi}(t, t_w)$ decays very slowly for systems in the ordered stripe phase [Fig. 3(a)], with only a slight dependence on t_w for large differences $t - t_w$.

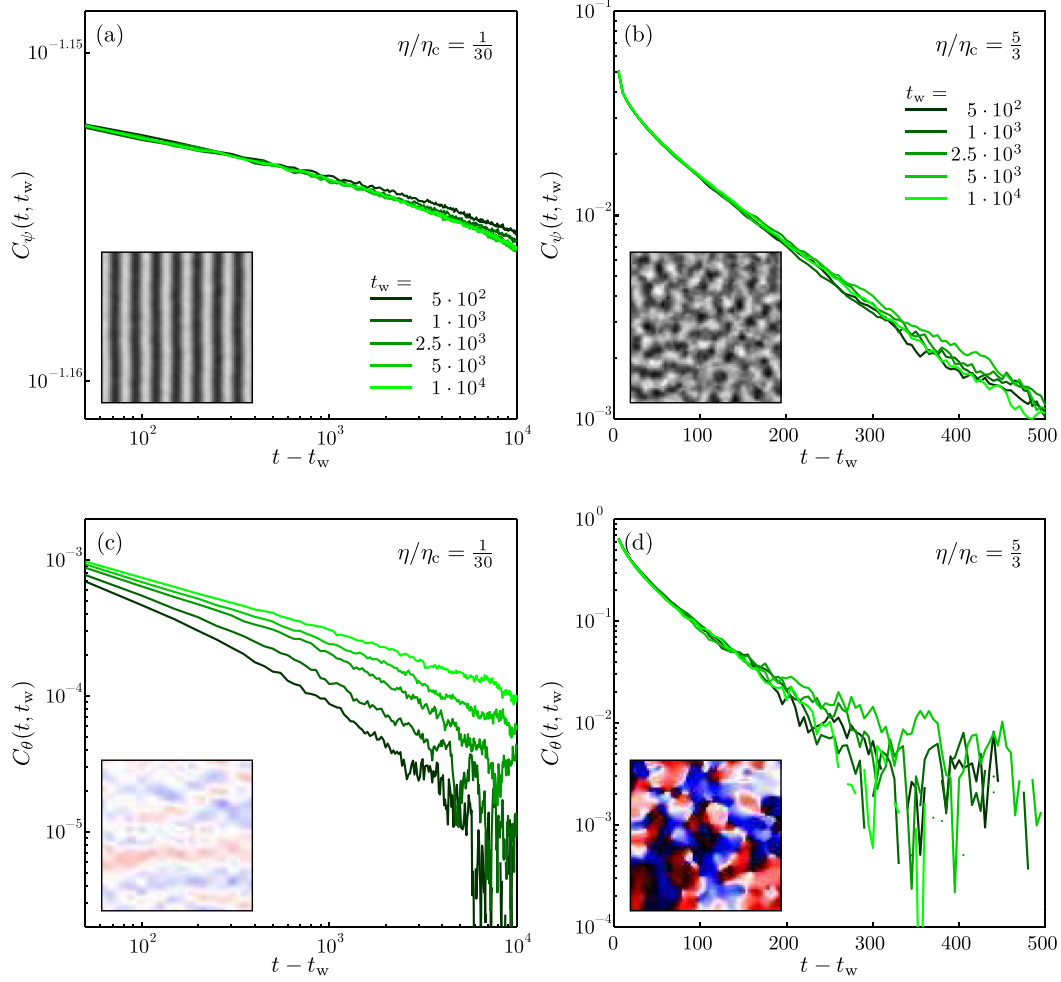


FIG. 3. (Color online) Dependence of relaxations on waiting time t_w and noise strength η . The (a),(b) concentration autocorrelation function $C_\psi(t, t_w)$ is compared to the (c),(d) orientation autocorrelation function $C_\theta(t, t_w)$. Both functions are plotted as a function of the time difference $t - t_w$ for different waiting times t_w , with $t_w = 5 \times 10^2, 10^3, 2.5 \times 10^3, 5 \times 10^3$ and 10^4 (from dark to bright). Data for the two different noise strengths below and above η_c are shown as indicated. $C_\psi(t, t_w)$ exhibits a very slow decay and no dependence on the waiting time (a). In contrast, $C_\theta(t, t_w)$ decreases more slowly for longer waiting times (c). Both functions decay exponentially for $\eta > \eta_c$ (b), (d). The insets show cropped snapshots (size 70×70) of the concentration field $\psi(\mathbf{r}, t)$ and the orientation field $\theta(\mathbf{r}, t)$ for $t = 10^4$, respectively, demonstrating the absence of long-range order for $\eta > \eta_c$.

For $\eta/\eta_c = 5/3$, $C_\psi(t, t_w)$ decreases much faster, namely, exponentially with $t - t_w$, and it is independent of the waiting time [Fig. 3(b)]. In contrast, the orientation autocorrelation function $C_\theta(t, t_w)$ decays approximately as a power law of $t - t_w$ for systems in the ordered state [Fig. 3(c)], and there is a pronounced dependence on t_w . The longer the waiting time t_w , the slower the relaxation becomes. Conversely, for $\eta > \eta_c$, we observe an exponential decay in $C_\theta(t, t_w)$, and no dependence on the waiting time is discernible [Fig. 3(d)]. From these results, we conclude that for $\eta > \eta_c$, the system is in a stationary state even on short time scales, as evidenced by the correlation functions depending only on the time difference, $t - t_w$. For $\eta < \eta_c$, the stripe system exhibits a slow dynamics with clear indications of aging behavior, which we will analyze below.

C. Scaling of orientation correlations

A common scaling form for the two-time correlation functions $C(t, t_w)$, referred to as simple aging [58], is given by

$$C(t, t_w) \sim t_w^{-b} f(t/t_w), \quad (3)$$

where $f(t/t_w)$ is a scaling function and b is a non-negative exponent [14,59,60]. To check for the scaling form given by Eq. (3), we plot $C_\theta(t, t_w)$ as a function of t_w while keeping the ratio $t/t_w = 3/2$ constant. Figure 4(a) shows the resulting plots for the noise strengths $\eta/\eta_c = \frac{1}{30}, \frac{1}{3},$ and $\frac{2}{3}$, ranging from very small noise strengths to values close to η_c . For $t_w \gtrsim 1000$, $C_\theta(t, t_w)$ exhibits a power-law behavior in t_w . Varying the noise strength causes a change in the magnitudes,

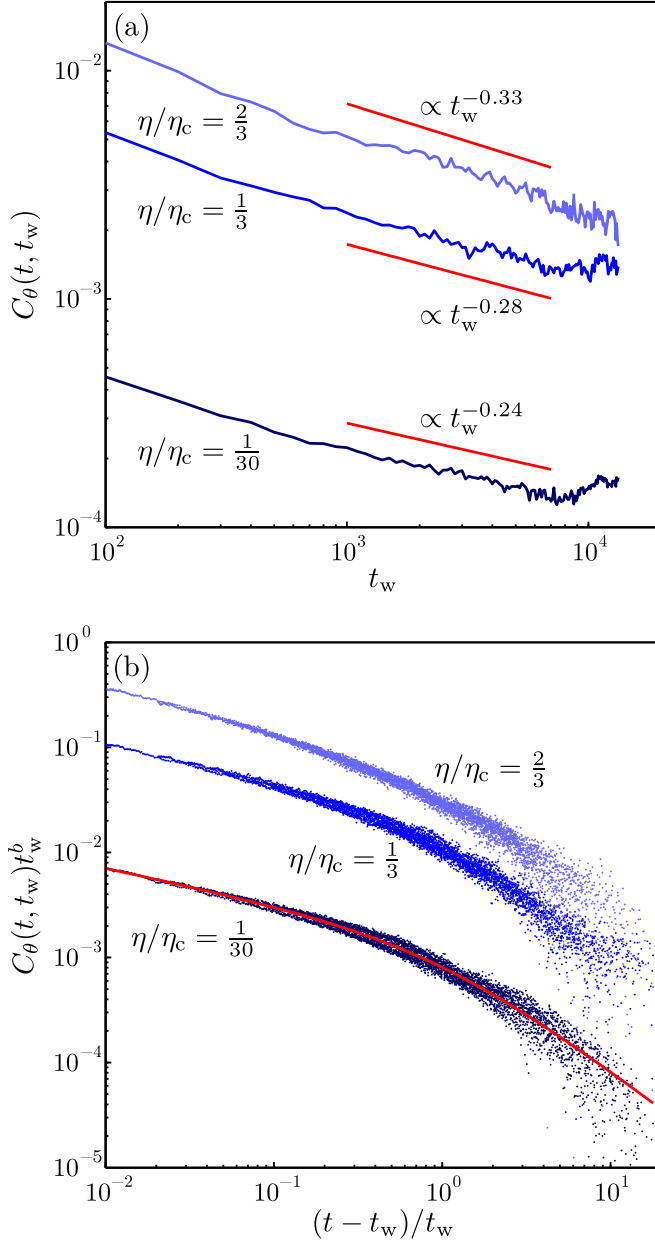


FIG. 4. (Color online) Scaling form of the orientation autocorrelation function. (a) $C_\theta(t, t_w)$ as a function of t_w for a constant ratio $t/t_w = 3/2$ and different noise strengths. The straight red line represents a power law. (b) The rescaled orientation correlation function $C_\theta(t, t_w)t_w^b$ plotted vs $(t - t_w)/t_w$. The red line is the fit function $f_2(x)$ (see text). The waiting time $t_w \in [10^3, 2 \times 10^4]$.

but only slightly affects the exponent. The least-squares fitting of the data yields the values $b = 0.24, 0.28,$ and 0.33 for the noise strengths $\eta/\eta_c = \frac{1}{30}, \frac{1}{3},$ and $\frac{2}{3}$, respectively. We now obtain the scaling function $f_\theta(t/t_w)$ by computing the rescaled correlation function $C_\theta(t, t_w)t_w^b$, which we plot as a function of $(t - t_w)/t_w$ [Fig. 4(b)]. For each of the values for η , we find a collapse in the data, thereby confirming the scaling relation given in Eq. (3). Regarding the form of the scaling function $f_\theta(t/t_w)$ describing the orientation correlation function, we consider two candidates: a stretched exponential, $f_1(x) \propto \exp[-\alpha_1(x - 1)^{\beta_1}]$, and a product of power laws,

$f_2(x) \propto x^{-\alpha_2}(x - 1)^{-\beta_2}$. Both functions $f_1(x)$ (with $\alpha_1 = 3.4, \beta_1 = 0.22$) and $f_2(x)$ (with $\alpha_2 = 0.89, \beta_2 = 0.34$) fit the data for $\eta/\eta_c = \frac{1}{30}$ equally well in the numerically accessible range [Fig. 4(b)]. However, only $f_2(x)$ has a diverging average relaxation time and also exhibits the expected power-law behavior as $x \rightarrow \infty$ [14,58]. We note that the data for $\eta/\eta_c = \frac{1}{3}$ and $\frac{2}{3}$ can also be fitted with both $f_1(x)$ and $f_2(x)$, with similar fit parameters as for $\eta/\eta_c = \frac{1}{30}$. The scaling form given by Eq. (3) with $b > 0$ is usually associated with the dynamics at a critical point [14,59]. In our case, however, the scaling relation holds for a wide range of noise strengths, in particular for $\eta \ll \eta_c$. Therefore, the behavior of the correlation functions is not related to the ODT, but instead is an intrinsic property of the ordered stripe phase.

Another aspect of critical systems in equilibrium is the presence of spatial correlations at all length scales. Starting from an ordered state, this implies a growing length scale. In Fig. 5(a), we plot cuts through the spatial correlation function $C_\theta(\mathbf{r}, t) \equiv C_\theta(r_\perp, r_\parallel, t)$ perpendicular to the stripe pattern. For short and intermediate times, the correlation function is short range and can be fitted with an exponential $\propto \exp(-r_\perp/\xi_\theta)$. The resulting orientational correlation length $\xi_\theta(t)$ is plotted in Fig. 5(b), showing a time dependence $\xi_\theta \propto t^z$, with the dynamic exponent $z = 2$ independent of the noise strength. This value is found in many nonconserved phase ordering systems [13], especially the two-dimensional (2D) XY model [61]. The nature of orientation correlations changes from being exponential at earlier times $t \lesssim 10^4$ to a power-law behavior $C_\theta(r_\perp, t) \propto r_\perp^{-c}$ for times $t \gtrsim 10^5$ [Fig. 5(c)]. The exponent c depends on the noise strength, with $c \approx 0.3$ for $\eta/\eta_c = \frac{1}{30}$ and $c \approx 0.5$ for a larger noise strength, $\eta/\eta_c = \frac{1}{3}$. The values of c we observe at $t = 5 \times 10^5$ might not be those of the infinite time limit, as there is still a slow relaxation in progress at the longest times considered in our study. In contrast, spatial correlations are short range in the direction parallel to the stripe pattern and exhibit a fast decay within a distance $r_\parallel \approx \lambda$ [Fig. 5(d)]. Their overall shape shows only a weak dependence on time. These findings of increasing orientation correlations perpendicular to the stripes are in agreement with the elongated orientational domains visible in Fig. 2(b).

IV. DISCUSSION

To elucidate the mechanism leading to a slow dynamics in the stripe system, we now compare our results to other nonequilibrium systems. A rugged free-energy landscape has been identified in Eq. (2) for $d = 3$ [20] and $d = 2$ [62], leading to a glass transition of the stripe system. These results could, in principle, provide an explanation for the aging effects we observe. We address this question by performing quenches to $\eta = 0$ of systems which have evolved over a time t_w at finite η , which causes the systems to perform a gradient descent towards the nearest minimum of the free energy $\mathcal{F}[\psi]$ [29]. The presence of many local minima should manifest itself as an arrest of the dynamics some time after the quench, in a state referred to as an inherent structure [63] in the language of molecular glass formers. However, we find that for quenches from $\eta < \eta_c$ to $\eta = 0$, the system always approaches a perfect

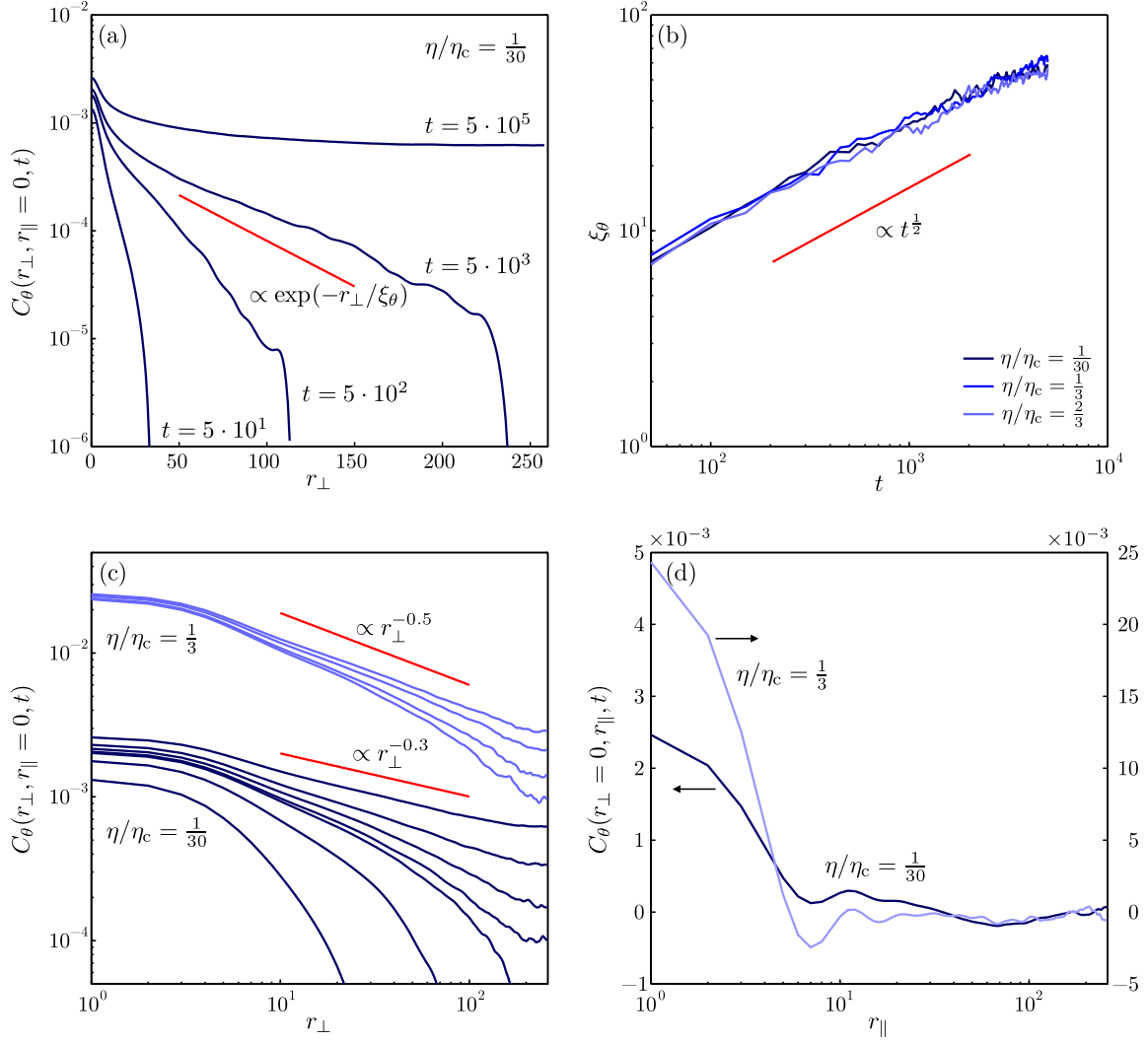


FIG. 5. (Color online) Growth of spatial orientation correlations at early and late times. (a) Spatial orientation correlation function perpendicular to the stripes at early times $t = 5 \times 10^1$, 5×10^2 , and 5×10^3 as well as for $t = 5 \times 10^5$ (bottom to top). An exponential function is plotted as a guide to the eye. (b) Orientational correlation length $\xi_\theta(t)$. The red line represents a power law with an exponent $\frac{1}{2}$. (c) $C_\theta(r_\perp, r_\parallel = 0, t)$ at late times $t = 5 \times 10^5$, 10^5 , 2×10^4 , and 10^4 ($\eta/\eta_c = \frac{1}{3}$, top to bottom). For $\eta/\eta_c = \frac{1}{30}$, data for $t = 5 \times 10^5$, 10^5 , 2×10^4 , 10^4 , 5×10^3 , 5×10^2 , and $t = 5 \times 10^1$ are shown. The straight red lines correspond to power laws with the indicated exponents. (d) Spatial orientation correlation function parallel to the stripes at $t = 5 \times 10^5$. The arrows indicate the corresponding ordinate.

pattern of parallel stripes, with the same wave number as that of the initial condition. The dynamics after the quench is slow, which is manifest in the autocorrelation function $C_\theta^Q(t, t_w)$, which decays with a power law in $t - t_w$, characterized by the exponent b_Q [Fig. 6(a)]. These findings exclude a complex free-energy landscape as the cause for aging. The emergence of the many metastable states found for Eq. (2) in Ref. [20] seems to be related to the presence of topological defects [64]. Yet it has been recognized that aging can also occur in partially flat energy landscapes [12,65].

Stripe-forming systems are often compared to 2D smectic systems [66], since they possess orientational and translational degrees of freedom. Toner and Nelson [67] found that 2D smectics are described by an effective nematic free energy due to a finite density of dislocations. At long wavelengths,

the nematic model becomes isotropic and equivalent to the 2D XY model [68,69]. Although we study an ordered (and therefore anisotropic) stripe-forming system without topological defects, we nevertheless observe a number of similarities with the XY model. The latter is critical for the whole range of temperatures $0 < T < T_{KT}$, where T_{KT} is the Kosterlitz-Thouless transition temperature [69], and the autocorrelation function after a quench from ordered initial conditions shows aging with the same form we find for $C_\theta(t, t_w)$ [Eq. (3)] [70], but with a different scaling function. Both systems exhibit a growing length scale with the dynamic exponent $z = 2$ [61], which, however, is confined to the r_\perp direction for the stripe system [Fig. 5(b)]. Similarly, the spatial correlation function decays as a power law of r_\perp at late times, whereas the XY model shows isotropic power-law correlations

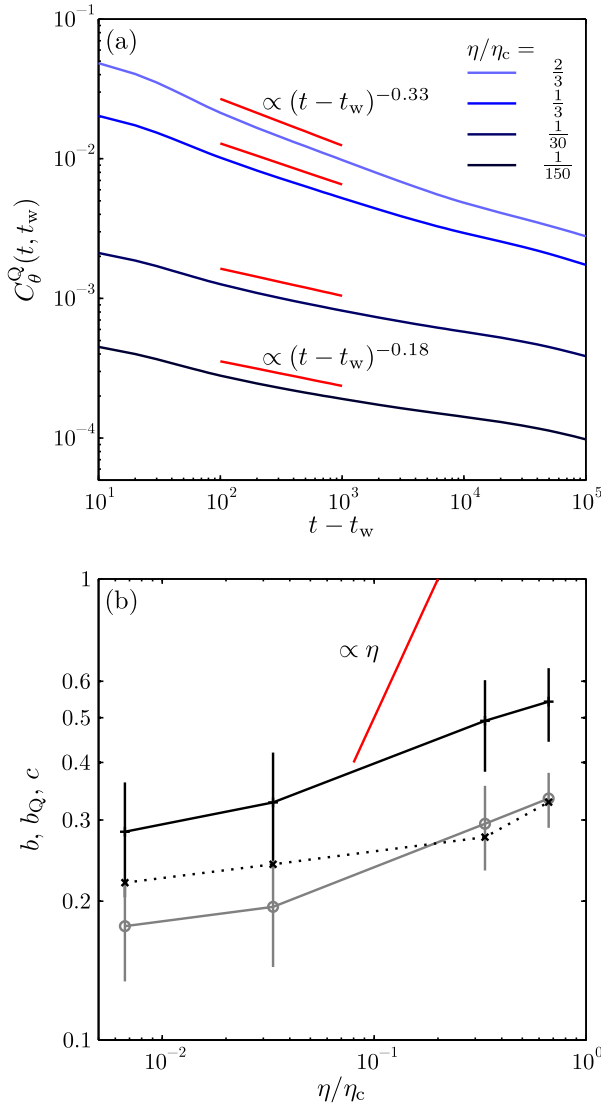


FIG. 6. (Color online) Orientation correlations after a quench to $\eta = 0$. Stripe patterns which had previously evolved at a finite noise strength η for a time $t_w = 5 \times 10^5$ were quenched to $\eta = 0$. (a) The orientation autocorrelation function $C_\theta^Q(t, t_w)$ is plotted on a double logarithmic scale as a function of the time $t - t_w$ after the quench for different noise strengths η . The red lines are power laws fitted for $10^2 \leq t - t_w \leq 10^3$, with the resulting exponents growing from 0.18 for $\eta/\eta_c = \frac{1}{150}$ to 0.33 for $\eta/\eta_c = \frac{2}{3}$. (b) Dependence of the exponents b (\times), b_Q (\circ), and c ($+$), obtained from temporal and spatial correlation functions, on the noise strength. For comparison, the red line represents a linear dependence on η . For b_Q and c , the error bars represent the standard deviation over 40 realizations of the system. The exponent c has been obtained from a fit to the sample average [Fig. 4(a)].

in equilibrium [69]. The distribution function of the order parameter of the XY model has a form characteristic for critical systems for $0 < T < T_{KT}$ [71], while we see asymptotic convergence to this distribution only for the noise strength η approaching zero [26]. Finally, quenching the XY model from $T < T_{KT}$ to zero temperature results in a slow relaxation, with a power-law decay of the autocorrelation function [72], similar to our findings [Fig. 6(a)]. In the XY model, the quench dynamics, the spatial correlations, as well as the decay of the autocorrelation function show power-law behavior with multiples of a single exponent, which depends linearly on the temperature. In the stripe-forming system, we also observe power-law behavior, but the exponents depend nonlinearly on the noise strength η [Fig. 6(b)] and are larger than in the XY model [73,74]. Furthermore, while the exponents b_Q and c seem to be related by a constant factor of approximately 5/3, the exponent b varies differently with η . These observations imply that the stripe-forming system belongs to a different universality class than the 2D XY model.

Preliminary simulation results [26] show that stripes described by the Swift-Hohenberg equation [27], 2D hexagonal and 3D lamellae-forming systems also exhibit aging dynamics, indicating that this might also be a property of other modulated phases [23]. Our results could be experimentally tested in systems such as thin films of block copolymers, where the dynamics of stripe patterns can be imaged [16,75,76] and similar orientation patterns as those shown in Fig. 2(b) have been observed [57]. Another candidate is Rayleigh-Bénard convection, where some effects of thermal noise have already been demonstrated [77].

V. CONCLUSION

In summary, we report on aging behavior in an ordered stripe system, caused by small angle orientation fluctuations. This is an intrinsic mechanism for the disordering of a prototype of a modulated phase without topological defects. For a wide range of noise strengths, the system exhibits a nonequilibrium relaxation and shows signs of criticality, as evidenced by the spatiotemporal correlations of the local stripe orientation. Our discovery of aging raises the question of whether stripe phases can reach equilibrium and how they might do so.

ACKNOWLEDGMENTS

Fruitful discussions with H. Chaté, M. C. Cross, L. F. Cugliandolo, and J. J. Toner are gratefully acknowledged.

- [1] M. C. Cross and P. C. Hohenberg, *Rev. Mod. Phys.* **65**, 851 (1993).
- [2] I. W. Hamley, *The Physics of Block Copolymers* (Oxford University Press, Oxford, 1998).
- [3] K. De'Bell, A. B. MacIsaac, and J. P. Whitehead, *Rev. Mod. Phys.* **72**, 225 (2000).

- [4] V. J. Emery, S. A. Kivelson, and J. M. Tranquada, *Proc. Natl. Acad. Sci. USA* **96**, 8814 (1999).
- [5] E. Bodenschatz, W. Pesch, and G. Ahlers, *Annu. Rev. Fluid Mech.* **32**, 709 (2000).
- [6] P. M. Chaikin and T. C. Lubensky, *Principles of Condensed Matter Physics* (Cambridge University Press, Cambridge, 1995).

- [7] L. Cugliandolo, in *Slow Relaxations and Nonequilibrium Dynamics in Condensed Matter*, Les Houches, Vol. 77, edited by J.-L. Barrat, M. Feigelman, J. Kurchan, and J. Dalibard (Springer, Berlin, 2003).
- [8] P. G. Debenedetti and F. H. Stillinger, *Nature (London)* **410**, 259 (2001).
- [9] L. Berthier and G. Biroli, *Rev. Mod. Phys.* **83**, 587 (2011).
- [10] A. P. Young, *Spin Glasses and Random Fields* (World Scientific, Singapore, 1998).
- [11] K. Binder and W. Kob, *Glassy Materials and Disordered Solids* (World Scientific, Hackensack, NJ, 2005).
- [12] L. F. Cugliandolo, J. Kurchan, and G. Parisi, *J. Phys. I (France)* **4**, 1641 (1994).
- [13] A. J. Bray, *Adv. Phys.* **43**, 357 (1994).
- [14] M. Zannetti, in *Kinetics of Phase Transitions*, edited by S. Puri and V. K. Wadhawan (CRC, Boca Raton, FL, 2009).
- [15] J. J. Christensen and A. J. Bray, *Phys. Rev. E* **58**, 5364 (1998).
- [16] C. Harrison, D. H. Adamson, Z. Cheng, J. M. Sebastian, S. Sethuraman, D. A. Huse, R. A. Register, and P. M. Chaikin, *Science* **290**, 1558 (2000); C. Harrison, Z. Cheng, S. Sethuraman, D. A. Huse, P. M. Chaikin, D. A. Vega, J. M. Sebastian, R. A. Register, and D. H. Adamson, *Phys. Rev. E* **66**, 011706 (2002).
- [17] H. Qian and G. F. Mazenko, *Phys. Rev. E* **67**, 036102 (2003).
- [18] H. R. Schober, E. Allroth, K. Schroeder, and H. Müller-Krumbhaar, *Phys. Rev. A* **33**, 567 (1986).
- [19] D. Boyer and J. Viñals, *Phys. Rev. E* **65**, 046119 (2002).
- [20] J. Schmalian and P. G. Wolynes, *Phys. Rev. Lett.* **85**, 836 (2000).
- [21] C.-Z. Zhang and Z.-G. Wang, *Phys. Rev. E* **73**, 031804 (2006).
- [22] S. Qi and Z.-G. Wang, *J. Chem. Phys.* **111**, 10681 (1999).
- [23] M. Seul and D. Andelman, *Science* **267**, 476 (1995).
- [24] P. C. Hohenberg and B. I. Halperin, *Rev. Mod. Phys.* **49**, 435 (1977).
- [25] T. Ohta and K. Kawasaki, *Macromolecules* **19**, 2621 (1986).
- [26] C. Riesch, G. Radons, and R. Magerle (unpublished).
- [27] J. Swift and P. C. Hohenberg, *Phys. Rev. A* **15**, 319 (1977).
- [28] S. A. Brazovskii, *Sov. Phys. JETP* **41**, 85 (1975) [*Zh. Eksp. Teor. Fiz.* **68**, 175 (1975)].
- [29] F. Liu and N. Goldenfeld, *Phys. Rev. A* **39**, 4805 (1989).
- [30] M. Bahiana and Y. Oono, *Phys. Rev. A* **41**, 6763 (1990).
- [31] I. W. Hamley, *Macromol. Theory Simul.* **9**, 363 (2000).
- [32] S. R. Ren and I. W. Hamley, *Macromolecules* **34**, 116 (2001).
- [33] S. R. Ren, I. W. Hamley, P. I. C. Teixeira, and P. D. Olmsted, *Phys. Rev. E* **63**, 041503 (2001).
- [34] Y. Xu, N. Xie, W. Li, F. Qiu, and A.-C. Shi, *J. Chem. Phys.* **137**, 194905 (2012).
- [35] N. Xie, W. Li, F. Qiu, and A.-C. Shi, *Soft Matter* **9**, 536 (2013).
- [36] M. Pinna and A. Zvelindovsky, *Eur. Phys. J. B* **85**, 210 (2012).
- [37] V. Weith, A. Krekhov, and W. Zimmermann, *J. Chem. Phys.* **139**, 054908 (2013).
- [38] S. C. Glotzer, E. A. Di Marzio, and M. Muthukumar, *Phys. Rev. Lett.* **74**, 2034 (1995).
- [39] J. J. Christensen, K. Elder, and H. C. Fogedby, *Phys. Rev. E* **54**, R2212 (1996).
- [40] A. W. Bosse, *Macromol. Theory Simul.* **19**, 399 (2010).
- [41] A. W. Bosse, *Phys. Rev. E* **85**, 042801 (2012).
- [42] P. N. Patrone and G. M. Gallatin, *Macromolecules* **45**, 9507 (2012).
- [43] U. Löw, V. J. Emery, K. Fabricius, and S. A. Kivelson, *Phys. Rev. Lett.* **72**, 1918 (1994).
- [44] P. Viot and G. Tarjus, *Europhys. Lett.* **44**, 423 (1998).
- [45] M. Grousson, G. Tarjus, and P. Viot, *Phys. Rev. E* **64**, 036109 (2001).
- [46] C. B. Muratov, *Phys. Rev. E* **66**, 066108 (2002).
- [47] J. W. Cahn, *Acta Metall.* **9**, 795 (1961).
- [48] K. R. Elder, J. Viñals, and M. Grant, *Phys. Rev. Lett.* **68**, 3024 (1992).
- [49] P. C. Hohenberg and J. B. Swift, *Phys. Rev. A* **46**, 4773 (1992).
- [50] S. Komura, J.-i. Fukuda, and G. C. Paquette, *Phys. Rev. E* **53**, R5588 (1996).
- [51] T. Taneike and Y. Shiwa, *J. Phys.: Condens. Matter* **11**, L147 (1999).
- [52] L. Q. Chen and J. Shen, *Comput. Phys. Commun.* **108**, 147 (1998).
- [53] N. Becker and G. Ahlers, *J. Stat. Mech: Theory Exp.* (2006) P12002.
- [54] J. v. d. Weijer, L. J. v. Vliet, P. W. Verbeek, and M. v. Ginkel, *IEEE Trans. Pattern Anal. Mach. Intell.* **23**, 1035 (2001).
- [55] Y. Shiwa, T. Taneike, and Y. Yokojima, *Phys. Rev. Lett.* **77**, 4378 (1996).
- [56] See Supplemental Material at <http://link.aps.org/supplemental/10.1103/PhysRevE.90.052101> for videos showing the evolution of the concentration field $\psi(\mathbf{r}, t)$ and orientation field $\theta(\mathbf{r}, t)$.
- [57] M. R. Hammond and E. J. Kramer, *Macromolecules* **39**, 1538 (2006).
- [58] M. Henkel and M. Pleimling, *Non-equilibrium Phase Transitions* (Springer, Dordrecht, 2010), Vol. 2.
- [59] C. Godrèche and J. M. Luck, *J. Phys.: Condens. Matter* **14**, 1589 (2002).
- [60] P. Calabrese and A. Gambassi, *J. Phys. A: Math. Gen.* **38**, R133 (2005).
- [61] A. J. Bray, A. J. Briant, and D. K. Jervis, *Phys. Rev. Lett.* **84**, 1503 (2000).
- [62] A. C. Ribeiro Teixeira, D. A. Stariolo, and D. G. Barci, *Phys. Rev. E* **87**, 062121 (2013).
- [63] F. H. Stillinger and T. A. Weber, *Science* **225**, 983 (1984).
- [64] H. Westfahl, J. Schmalian, and P. G. Wolynes, *Phys. Rev. B* **64**, 174203 (2001).
- [65] J. Kurchan and L. Laloux, *J. Phys. A: Math. Gen.* **29**, 1929 (1996).
- [66] P. de Gennes and J. Prost, *The Physics of Liquid Crystals*, International Series of Monographs on Physics (Clarendon, Oxford, 1995).
- [67] J. Toner and D. R. Nelson, *Phys. Rev. B* **23**, 316 (1981).
- [68] D. R. Nelson and R. A. Pelcovits, *Phys. Rev. B* **16**, 2191 (1977).
- [69] J. M. Kosterlitz and D. J. Thouless, *J. Phys. C* **6**, 1181 (1973).
- [70] L. Berthier, P. C. W. Holdsworth, and M. Sellitto, *J. Phys. A: Math. Gen.* **34**, 1805 (2001).
- [71] S. T. Bramwell, K. Christensen, J.-Y. Fortin, P. C. W. Holdsworth, H. J. Jensen, S. Lise, J. M. López, M. Nicodemi, J.-F. Pinton, and M. Sellitto, *Phys. Rev. Lett.* **84**, 3744 (2000).
- [72] A. D. Rutenberg and A. J. Bray, *Phys. Rev. E* **51**, R1641 (1995).
- [73] J. M. Kosterlitz, *J. Phys. C* **7**, 1046 (1974).
- [74] S. Abriet and D. Karevski, *Eur. Phys. J. B* **37**, 47 (2004).
- [75] A. Knoll, K. S. Lyakhova, A. Horvat, G. Krausch, G. J. A. Sevink, A. V. Zvelindovsky, and R. Magerle, *Nat. Mater.* **3**, 886 (2004).
- [76] L. Tsarkova, A. Knoll, and R. Magerle, *Nano Lett.* **6**, 1574 (2006).
- [77] J. Oh and G. Ahlers, *Phys. Rev. Lett.* **91**, 094501 (2003).